Electronic Supplementary information

Crystal phase-dependent optical properties of CoMn-based spinel oxides for solar thermal conversion

Huilan Ma,[IIa]shengyang Wang,[IIa] Qi Ye, [ab] Longfei Guo, [a]Entao Wang, [a]Jun Li, [a]and Can Li [*ab]

a. .State Key Laboratory of Catalysis, Dalian Institute of Chemical Physics, Chinese Academy of Sciences, Dalian National Laboratory for Clean Energy, Dalian 116023, China. University of Chinese Academy of Sciences, Beijing 100049, China
E-mail:canli@dicp.ac.cn
b. University of Chinese Academy of Sciences, Beijing 100049, China.

Table of contents

3. Supplementary Tables

1. Experimental details

Materials characterization

X-ray diffractometer (XRD) tests were performed on a SmartLab diffractometer using a Cu Kα radiation source (λ = 1.54056 Å) to determine crystal structures. Raman spectra was collected on a Renishaw inVia Raman microscope (λ = 532 nm) with the laser intensity of 0.2 mW. The morphologies were characterized on a scanning electron microscope (SEM, FEI Quanta 200F). The element contents of the samples were identified by inductively coupled plasma mass spectrometry (ICP-MS, ICPS-8100) and verified by energy-dispersive spectroscopy (EDS, JSM-7900F). The lattice of the sample was further verified by high-resolution transmission electron microscopy (HRTEM, HT7700). The valence state of the sample was characterized by X-ray photoelectron spectroscopy XPS (ESCALAB250xi). The charge effect was calibrated by using the binding energy of C1s (284.6 eV) to reduce the sample charging effect. The UV-vis-IR diffuse reflection spectra of thin films and powder samples were carried out on Cary 5000 with integrating sphere. The Pore size of samples were measured by ASAP2020.The thickness of films and coatings was tested with Dektak 150. During photothermal conversion tests, the surface temperature was imaged by IR camera (Fluke Thermography). Refractive index and extinction coefficient were obtained on an Ellipsometer (FQTH-100).

Films preparation by spin coating

Precursor solution preparation

Pluronic P123 (20 g) and cetyltrimethylammonium bromide (CTAB, 6.28 g) were added to 100 mL deionized water, and the solution was heated at 50 °C to dissolve the polymer. $Co(NO_3)_2 \cdot 6H_2O$ and $Mn(NO_3)_2 \cdot 4H_2O$ with an appropriate metal ion ratio (Co/Mn = 0.5, 1.0, and 2.0) were mixed in the above polymer solution (5 mL) with magnetic stirring at room temperature for 12 h.

Spin coating

1 mL of precursor solution was spin-coated on the quartz glass substrate with the assistance of a spin coater (rpm at 3000 for 30 s). Then, the spin-coated substrate was calcinated at 600 °C for 2 h (2 °C/min).

Synthesis of CoMn-based spinel oxide powder

Spinel oxide $Co_xMn_{3-x}O_4$ (x = 0.5–2) was synthesized by the sol-gel method. Typically, ethylenediaminetetraacetic acid (EDTA) and citric acid (CA) were used as chelating units. The molar ratio of total molar amount of metal salt/EDTA/CA is 2:2:3. Firstly, a stoichiometric $Co(NO_3)_2$•$4H_2O$ and $Mn(NO_3)_2$•$4H_2O$ were dissolved in 150 mL deionized water with magnetic stirring at room temperature. After the metal salt was dissolved, citric acid and EDTA were added to form a homogeneous solution with magnetic stirring at room temperature. Afterward, the solution was stirred for 1 h at room temperature. Then, ammonia was added to adjust the pH between 6 and 8 until the solution was clarified. Afterward, 100 mL of ethanol was added. The resulting solution was stirred and heated at 190 ℃ to obtain the sol, which was later converted into thick gel. The gel was calcined at 300 ℃ (5 ℃/min) for 5 h in a muffle furnace under air atmosphere. Finally, the black powder was grinded and calcined at 600 ℃ for 20 h (5 ℃/min).

Coating preparation

The slurries were prepared by a ball-milling method. Specifically, 0.5 g of Co_2MnO_4 and $CoMn_2O_4$ powders were dissolved in 10 mL of 2 wt% solvent (PVB/isobutanol = 2:98) and then ball-milled for 3 h at 372 rpm. The absorber coatings on a stainless steel 316 plate were prepared by a spray method, where the thickness of films could be managed by controlling the spraying time.

Photothermal conversion efficiency of coatings

0.5 g of $CoMn_2O_4$ and Co_2MnO_4 powders were dissolved in 10 mL of ethanol and then ball-milled for 3 h. The ink obtained was used for spray coating on a Cu film. Then we conducted the photothermal tests of CoMn oxides films under irradiation of a concentrated Xe lamp (P = 2.058 W), which has an irradiation spectrum similar to solar irradiation.

Calculation Details

All the ground state properties are calculated using the Vienna Ab Initio Simulation Package (VASP). Electron–ion interactions are described by using the all electron projector augmented wave (PAW) method. The generalized gradient approximation (GGA) with the Perdew–Burke–Ernzerhof (PBE) exchange–correlation functional is used to approximate correlation of electrons within the many-body wave function. All calculations are performed using a cut-off energy of 520 eV with the 2 × 2 × 7 Monkhorst-Pack grid. The calculations are stopped until the force less than 0.01 eV/Å, and the energy convergence criterion is set to 10^{-6} eV.

2. Supplementary Figures

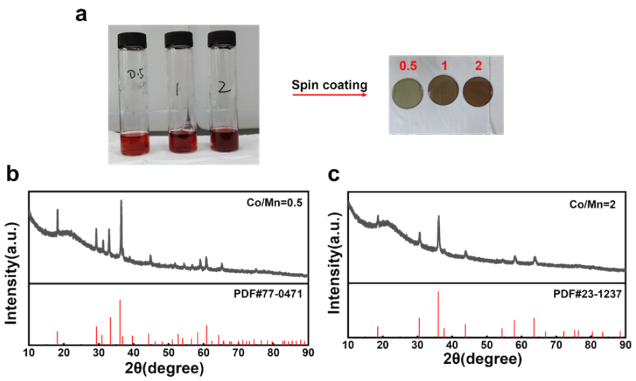

Figure S1. (a) Photos of spin-coating precursor solutions and of thin films with Co/Mn = 0.5, 1.0, and 2.0. (b, c) XRD patterns of the spinel films with Co/Mn = 0.5 and 2.0.

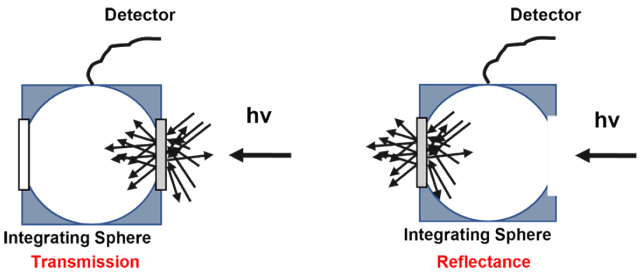

Figure S2. Transmission and reflection diagrams of the thin film, drawn with an integrating sphere method.

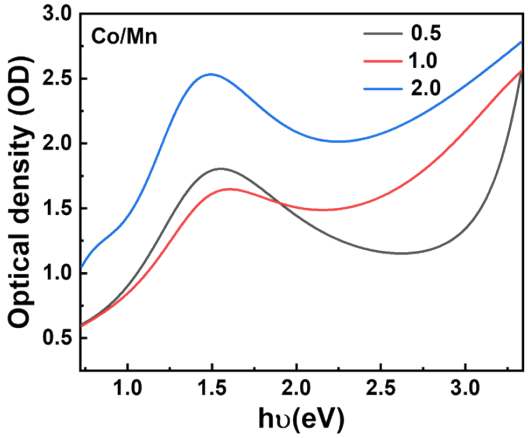

Figure S3. Optical density (OD) curves of the thin films with Co/Mn = 0.5, 1.0, and 2.0.

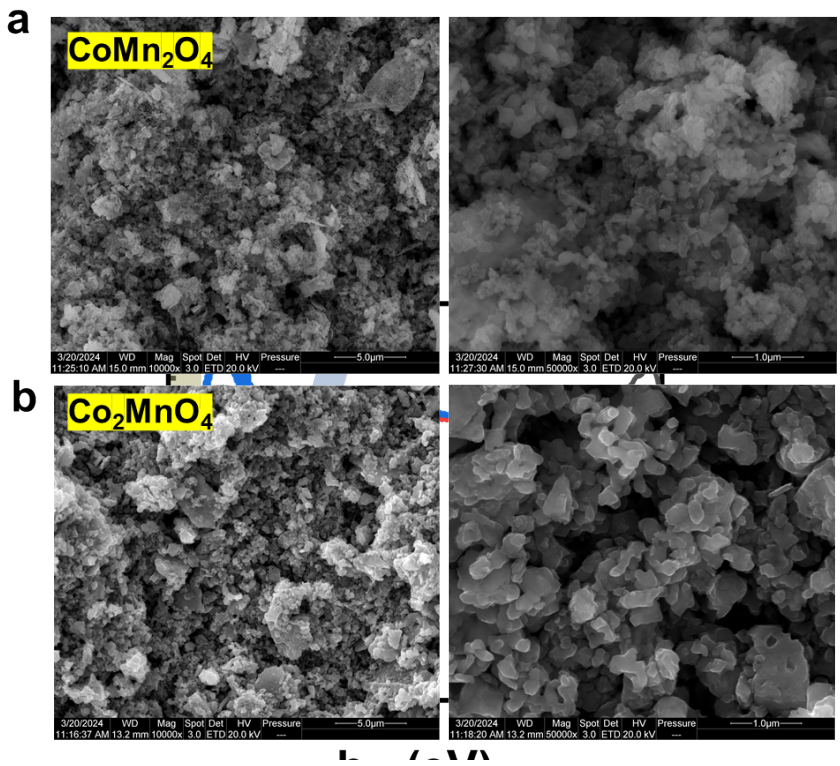

Figure S5. SEM characterization of $CoMn_2O_4$ and Co_2MnO_4. SEM images of (a) $CoMn_2O_4$ and (b) Co_2MnO_4.

tetrahedrally coordinated Co^{2+} ions between $^4A_2$ and $^4T_1$ bands. Peak ***B*** is attributed to CT transitions involving O^{2-} and octahedral cation ions.

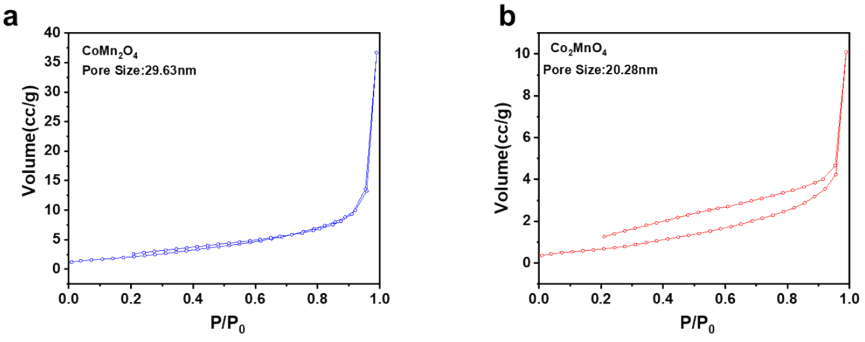

Figure S6. Pore size characterization of $CoMn_2O_4$ and Co_2MnO_4. (a) $CoMn_2O_4$ and (b) Co_2MnO_4

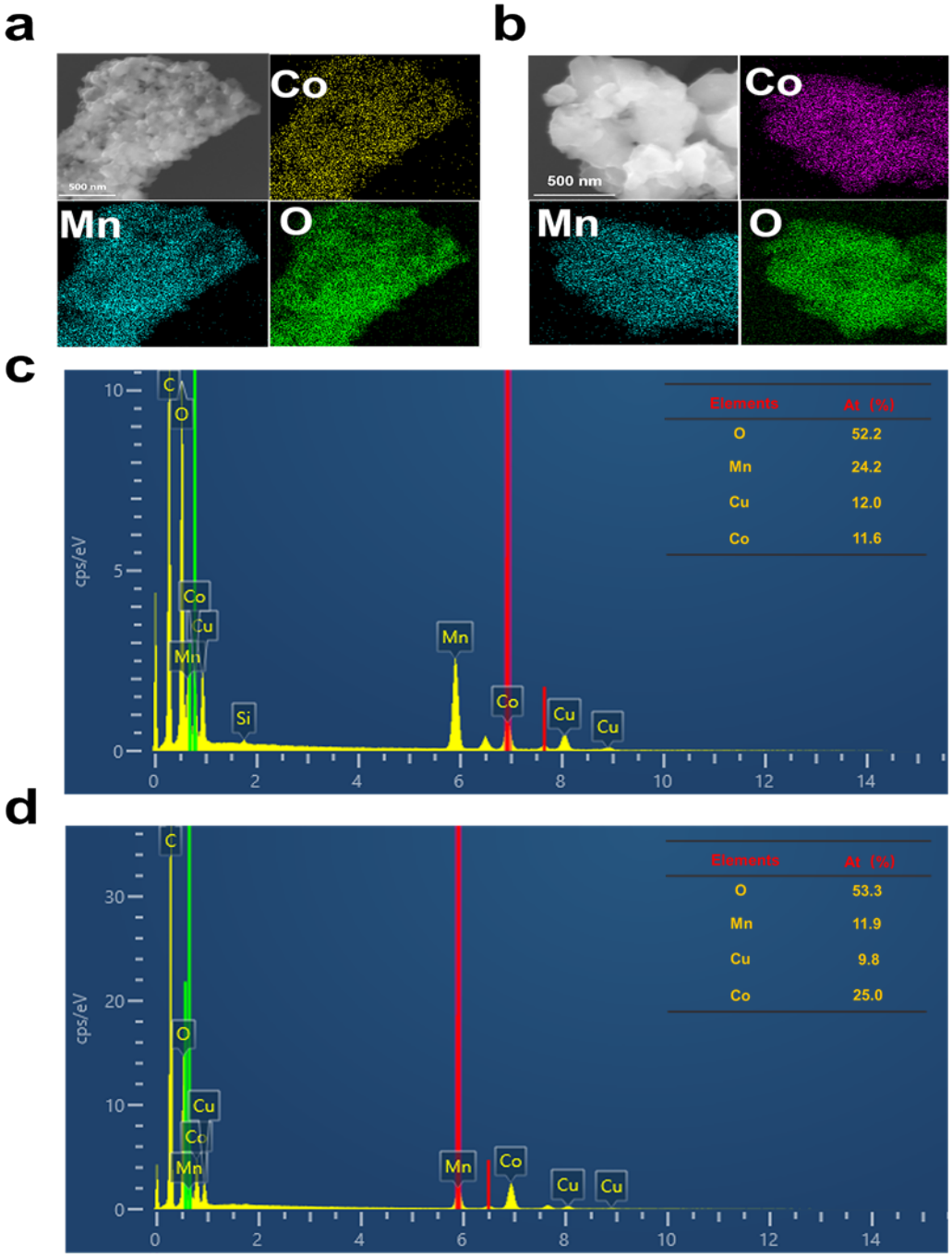

Figure S7. EDS characterization of $CoMn_2O_4$ and Co_2MnO_4. EDS images of (a) $CoMn_2O_4$ with a Co/Mn atom ratio of 0.5 and (b) Co_2MnO_4 with a Co/Mn atom ratio of 2.0. Atom ratio images of (c) $CoMn_2O_4$ and (d) Co_2MnO_4.

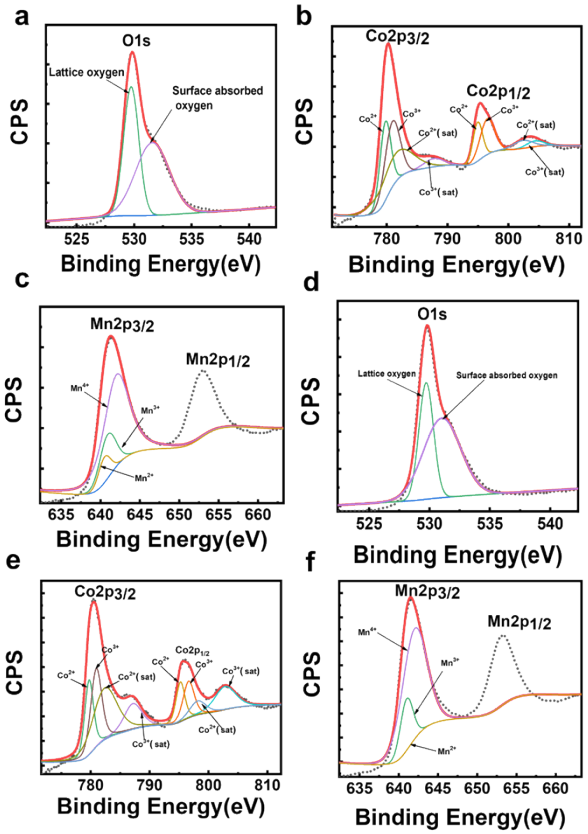

Figure S8. XPS characterization of $CoMn_2O_4$ and Co_2MnO_4. (a) O1s, (b) Co2p, and (c) Mn2p XPS spectra of $CoMn_2O_4$. (d) O1s, (e) Co2p, and (f) Mn2p XPS spectra of Co_2MnO_4.

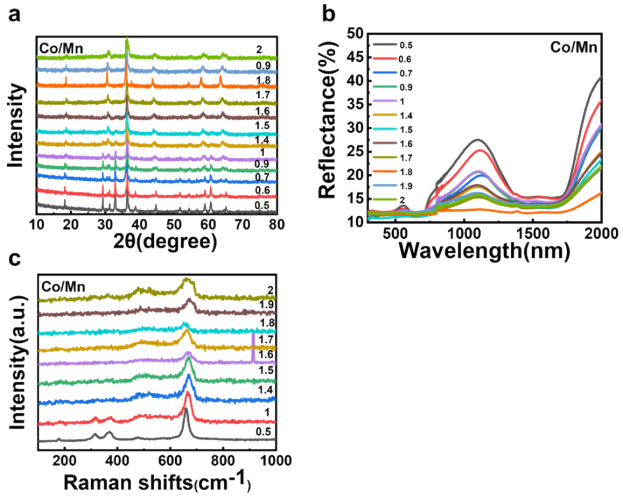

Figure S9. Structure and performance characterization of the films with different Co/Mn ratios. (a) XRD patterns, (b) reflectance and (c) Raman spectra of the films with Co/Mn ratio varying from 0.5 to 2.0.

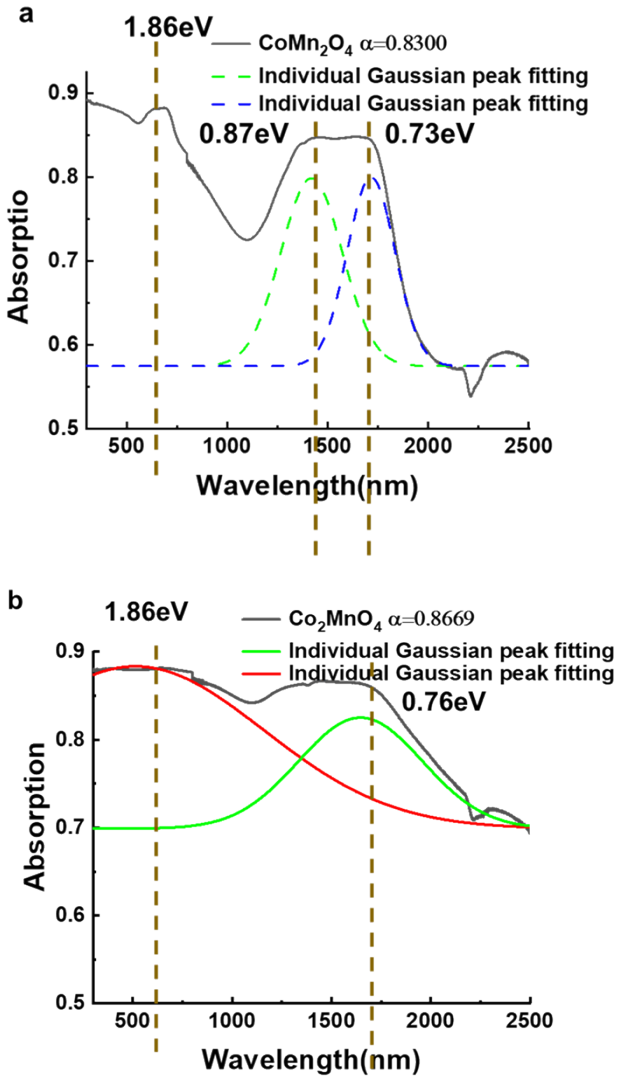

Figure S10. UV-vis-NIR spectra of (a) $CoMn_2O_4$ and (b) Co_2MnO_4.

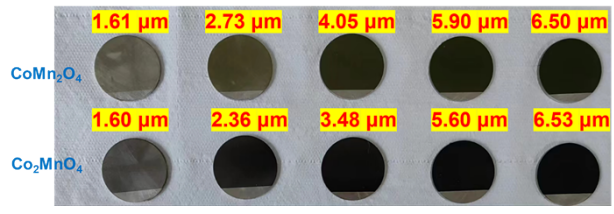

Figure S11. Photos of $CoMn_2O_4$ and Co_2MnO_4 coatings with different thicknesses.

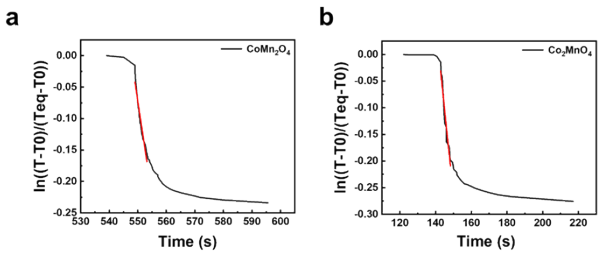

Figure S12. Fitting diagrams of thermal diffusivities of (a) $CoMn_2O_4$ and (b) Co_2MnO_4.

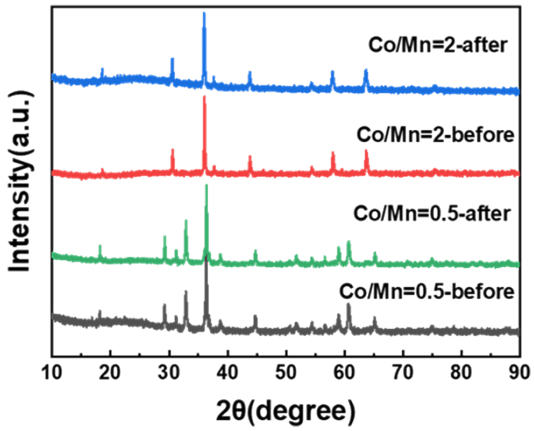

Figure S13. XRD patterns of the thin films with Co/Mn = 0.5 and 2.0 before and after three on/off cycles of photothermal conversion.

3. Supplementary Tables

Table S1. Thickness of the thin films with Co/Mn = 0.5, 1.0, and 2.0.

Atom Ratio	Thickness (nm)
0.5	118.6
1.0	120.2
2.0	115.1

Table S2. Rietveld refinement results of $CoMn_2O_4$ and Co_2MnO_4. Lattice parameters *a* and *c*, volume of the unit cell (V), and agreement

	$CoMn_2O_4$	Co_2MnO_4
Space group	$I\,4_1/\,amd$	Fd-3m
a(Å)	5.7	8.3
c(Å)	9.3	8.3
V(Å^3)	303	562
Rp(%)	12	15
Rwp(%)	17	19

Table S3. ICP characterization of $CoMn_2O_4$ and Co_2MnO_4. The Co/Mn atom ratios are 0.5 for $CoMn_2O_4$ and 2.0 for Co_2MnO_4.

	Co(mg/L)	Mn(mg/L)	Atom ratio (Co/Mn_{Actual})	Atom ratio (Co/Mn_{Theory})
Co/Mn=0.5	23.87	42.67	0.52	0.5
Co/Mn=2.0	50.38	23.02	2.04	2.0

Table S4. Absorbance of different Co/Mn ratios (from 0.5 to 2.0).

Ratio(Co/Mn)	Absorbance（%）
0.5	83
0.6	84
0.7	86
0.9	85
1.0	85
1.4	86
1.6	86
1.9	86
2.0	87

Table S5. Evaluation of photothermal efficiencies of $CoMn_2O_4$ and Co_2MnO_4.

	F(J/K/s)	Cp(J/g/K)	$\eta_{external}$(%)	η_0(%)
$CoMn_2O_4$	3.7E-3 3.6E-3 3.7E-3	0.385	61.5±1.2	69.4±1.3
Co_2MnO_4	5.2E-3 5.6E-3 5.5E-3	0.385	87.6±4.0	94.0 ± 4.3

$*mCp\frac{dT}{dt} + F(T - T_0) = 0$ $Pin \cdot \eta_{external} = F(T_{eq} - T_0)$ $\eta_0 = \eta/\alpha$